JOURNAL OF SOLID STATE CHEMISTRY 93, 503–509 (1991)

Synthesis and Crystal Structure of a New Antimony(III) Molybdate: $LiSbMo_2O_8$

K. H. LII* AND B. R. CHUEH†

*Institute of Chemistry, Academia Sinica, Nankang, Taipei, and †Department of Chemistry, National Chung Hsing University, Taichung, Taiwan, Republic of China

Received January 29, 1991; in revised form April 4, 1991

A new antimony(III) molybdate, $LiSbMo_2O_8$, was synthesized and its crystal structure was determined from single-crystal X-ray diffraction data. It crystallizes in the monoclinic space group $C2/c$ (No. 15) with $a = 21.640(6)$, $b = 4.9305(7)$, $c = 5.5448(6)$ Å, $\beta = 100.35(1)°$, $V = 582.0(2)$ Å^3, $Z = 4$, and $R = 0.026$. The structure consists of corrugated perovskite-like layers of markedly distorted MoO_6 octahedra with the Sb^{3+} and Li^+ ions segregated on opposite sides of each layer. The Sb^{3+} ion shows one-sided 4-coordination with four more oxygen atoms lying on the other side of the Sb^{3+} ion at considerably longer distances. The coordination around the Li^+ ion is octahedral. Alternatively, the structure is described as consisting of rutile-type slabs three edge-sharing octahedra thick, which are connected by the Sb^{3+} ions to form a three-dimensional framework. SCHLEGEL diagrams are used to help describe the arrangement of the next-nearest neighbors of the coordination polyhedra of Mo and Li. The structure is closely related to those of $SbNbO_4$, α-, and β-Sb_2O_4.

Introduction

Few antimony(III) molybdates are known at present. Sb_2MoO_6 (*1*) is structurally similar to Bi_2MoO_6 (*2*), which is related to those of the Aurivillius family of oxides consisting of intergrowths of BiO and perovskite layers. $Sb_2Mo_{10}O_{31}$ (*3*) consists of hexagonal tunnels formed by MoO_6 octahedra with the Sb^{3+} ions located in the tunnels. The average valence of Mo in $Sb_2Mo_{10}O_{31}$ is +5.6 and suggests that Mo^{6+} and Mo^{5+} are simultaneously present in the structure. Recently, we synthesized the potassium antimony(III) molybdenum oxide $KSbMo_2O_8$ (*4*). This new structure contains layers of antimony molybdate with the potassium cations between the layers. Each layer consists of Sb_2O_{10} dimers, MoO_5 polyhedra, and infinite chains formed by skew edge-shared MoO_6 octahedra. Since the nature of the alkali metal cation often plays an important role in the crystal structures, we began the synthesis from elements in place of potassium. The present paper is an extension of our interest in the system $ASb^{III}Mo^{VI}O$ (A = alkali metals) and describes the synthesis and crystal structure of $LiSbMo_2O_8$. The structure is markedly different from that of the corresponding potassium compound.

Experimental

Synthesis

Sb_2O_3 (99.9%), Li_2MoO_4 (99.9%), and MoO_3 (99.9%) were obtained from Cerac Inc. Because Li_2MoO_4 is hygroscopic, loading of the reactants was carried out in a glovebox which was flushed with nitrogen. Air-stable, olive crystals of $LiSbMo_2O_8$

0022-4596/91 $3.00

were obtained by heating a pressed pellet of Sb_2O_3, Li_2MoO_4, and MoO_3 (mole ratio 1 : 1 : 3) in a sealed silica tube at 510°C for 5 hr, slowly cooled at 2°C/hr to 470°C, maintained at 470°C for 2 days, and then furnace cooled to room temperature. The title compound was obtained as a single-phase material by heating the reaction mixture at 450°C for 4 days with an intermediate grinding. The powder X-ray pattern of the olive polycrystalline product, which was recorded at room temperature by using a Rigaku powder diffractometer with filtered copper radiation (λ = 1.5405 Å), can be completely indexed on a monoclinic cell with a = 21.655(5), b = 4.932(1), c = 5.546(1) Å, and β = 100.34(2)°. Silicon powder was mixed with the sample as an internal standard for calibrating the observed d-spacings. The indexed pattern of $LiSbMo_2O_8$ is given in Table I. Differential thermal analysis and powder X-ray diffraction showed that the compound partially decomposed on melting. The Li content of a single-phase product was checked by using an ICP-AE spectrometer after dissolving the sample in aqua regia. Anal. Calcd: 1.547%. Found: 1.55%.

TABLE I
X-RAY POWDER DIFFRACTION DATA FOR $LiSbMo_2O_8$

h	k	l	$2\theta_{obs}$ (deg)	d_{obs} (Å)	d_{calc} (Å)	I_{obs}
2	0	0	8.34	10.59	10.65	12.1
4	0	0	16.69	5.309	5.327	14.1
1	1	0	18.46	4.803	4.805	13.4
3	1	$\bar{0}$	21.96	4.045	4.051	13.6
1	1	$\bar{1}$	24.18	3.678	3.681	11.4
6	0	$\bar{0}$	25.09	3.546	3.551	37.8
3	1	$\bar{1}$	26.02	3.421	3.425	80.6
3	1	1	28.76	3.101	3.104	100.0
5	1	1	30.21	2.955	2.958	51.2
2	0	$\bar{2}$	32.35	2.765	2.765	14.0
0	0	2	32.82	2.727	2.728	31.4
8	0	0	33.65	2.661	2.664	29.0
5	1	1	34.17	2.621	2.624	16.7
0	2	0	36.42	2.465	2.466	12.9
4	2	$\bar{0}$	40.26	2.238	2.238	12.6
8	0	$\bar{2}$	42.99	2.102	2.104	20.8
6	2	0	44.77	2.022	2.026	17.9
6	0	2	45.42	1.995	1.997	20.0
0	2	$\bar{2}$	49.84	1.828	1.829	36.3
11	1	$\bar{1}$	50.56	1.803	1.804	39.3
3	1	$\bar{3}$	53.05	1.724	1.727	17.7
5	1	3	54.47	1.682	1.685	16.2
11	1	1	56.39	1.630	1.633	23.7
3	1	3	57.62	1.598	1.599	35.7
6	2	2	59.55	1.550	1.552	18.0

Single-Crystal X-Ray Structure Determination

An olive crystal having the dimensions 0.15 × 0.20 × 0.25 mm was selected for indexing and intensity data collection on an Enraf–Nonius CAD4 diffractometer at room temperature. The orientation matrix and unit cell parameters were determined by least-squares fit of 24 peak maxima with $18 < 2\theta < 27°$. The intensity data were corrected for Lorentz and polarization effects, but no absorption corrections were applied. Based on statistical analysis of intensity distribution and successful solution and refinement of the structure, the space group was determined to be $C2/c$. Direct methods (NRCVAX) were used to locate the Sb and Mo atoms, with the Li and O atoms being found from successive difference Fourier maps (5). Neutral-atom scattering factors and corrections for anomalous dispersion were taken from Cromer and Weber (6). The multiplicities of the Li, Sb, and Mo atoms were allowed to refine but did not deviate significantly from full occupancy. Therefore, the metal atom sites were considered to be fully occupied in subsequent refinement. The final cycles of full-matrix least-squares refinement including the secondary extinction coefficient converged at R = 0.026 and R_w = 0.034. The final difference map had a few ~1 e/Å^3 residuals near the heavy metal atoms.

Results and Discussion

Crystal data, intensity measurement, and structure refinement parameters are col-

TABLE II

CRYSTAL DATA, INTENSITY MEASUREMENT, AND REFINEMENT PARAMETERS FOR $LiSbMo_2O_8$

Crystal data	
Space group	$C2/c$ (No. 15)
a	21.640(6) Å
b	4.9305(7)Å
c	5.5448(6) Å
β	100.35(1)°
V	582.0(2) Å^3
Z	4
D_x	5.119 g/cm^3
Intensity measurement	
λ (Mo$K\alpha$)	0.70930 Å
$2\theta_{max}$	55°
Scan type	$\omega - (4/3)\theta$
Scan speed	8.24°/min
Scan width	$0.6° + 0.35° \tan\theta$
Standard reflections	530, 821, 421 (measured every 1 hr, no decay)
Structure solution and refinement	
No. of reflections included	667 ($I \geq 2.5\ \sigma(I)$)
No. of reflections measured	745
No. of parameters refined	53
$R(F)$	0.026
$R_w(F)$	0.034

lected in Table II. Table III contains the final atomic coordinates and thermal parameters. Selected bond distances and angles are given in Table IV. Motif of the mutual adjunction (*7*) and bond-order sums (*8*) are given in Table V. Bond-order sums for both the cations and the anions are in good accordance with their formal oxidation states. The six Mo–O bond distances can be divided into two groups: three shorter distances at 1.729–1.776 Å, and three longer ones at 2.074–2.208 Å *trans* to the shorter Mo–O bonds. The MoO_6 octahedron is strongly distorted and the octahedral distortion can be estimated by using the equation $\Delta = (1/6)\Sigma((R_i - \bar{R})/\bar{R})^2$, where R_i = an individual bond length and $\bar{R}$ = average bond length (*9*). The calculation result ($\Delta \times 10^4 = 112$) shows that the distortion is less pronounced than that in $KSbMo_2O_8$ ($\Delta \times 10^4 = 156$). According to Shannon (*9*), the deviation of $\bar{R}$ from a standard averaged value (1.920 Å) is proportional to Δ through an empirical coefficient, 3.73. We calculate $\bar{R}$ = 1.962 Å, identical to the average observed value. The octahedron containing Li^+ appears rather regular ($\Delta \times 10^4 = 1.5$). According to the maximum cation–anion distance (2.65 Å) for Sb^{3+}–O by Donnay and Allmann (*10*), the Sb atom in $LiSbMO_2O_8$ is bonded to four oxygen atoms at distances ranging from 2.01 to 2.21 Å. Therefore, the structure of $LiSbMo_2O_8$ is composed of strongly distorted MoO_6 octahedra, SbO_4 polyhedra, and LiO_6 octahedra. The four Sb–O bonds are on one side of the cation, showing the presence of a stereochemically active lone-pair orbital on Sb^{3+}. This orbital is largely made up of the Sb 5*s* orbital but includes some Sb 5*p* orbital character such that it extends away from the surrounding oxygen atoms. It is noted that 4 O(3) lie farther off on the other side of the Sb^{3+} ion at distances of 2.98 Å (2×) and 3.15 Å (2×). The next Sb–O distances are longer than 3.5 Å.

One can observe from the SCHLEGEL diagrams of a coordination polyhedron (C.P.) how the next-nearest neighbors are arranged in the structure (*11*). Figure 1 shows the C.P. of O around Mo in $LiSbMo_2O_8$. From the given Mo–O distances, the edge lengths, and the O–Mo–O angles, we see that the octahedron is markedly distorted. The four equatorial O atom vertices of a MoO_6 octahedron are shared with four MoO_6 octahedra and one LiO_6 octahedron. The remaining two vertices of the octahedron are shared with two SbO_6 polyhedra and one LiO_6 octahedron. It is noted that the shortest edge of a MoO_6 octahedron is shared with a neighboring LiO_6 octahedron. Figure 2 shows the C.P. of O around Li. It is apparent that two opposite edges are markedly shortened with respect to other edge lengths because of *trans*-edge sharing with MoO_6 octahedra. Each LiO_6 octahedron shares four equatorial O atom vertices with four LiO_6 octahedra and two MoO_6 octahedra. The axial vertices are shared with MoO_6 octahedra.

TABLE III

ATOMIC COORDINATES AND THERMAL PARAMETERS FOR $LiSbMo_2O_8$

Atom	x	y	z	B(iso) (Å^2)[a]
Sb	0	0.3087(1)	1/4	0.60(3)
Mo	0.36197(3)	0.2511(1)	0.2147(1)	0.63(3)
O(1)	0.8394(2)	0.452(1)	0.0432(9)	0.61(16)
O(2)	0.2902(2)	0.407(1)	0.2124(9)	0.71(17)
O(3)	0.1042(2)	0.048(1)	−0.0072(9)	0.62(16)
O(4)	0.5522(2)	0.091(1)	0.1190(9)	0.60(16)
Li	3/4	1/4	0	1.6(3)[b]

Anisotropic thermal parameters (Å^2 × 100)[c]

Atom	U_{11}	U_{22}	U_{33}	U_{12}	U_{13}	U_{23}
Sb	0.74(4)	0.86(4)	0.69(4)	0	0.16(2)	0
Mo	0.85(3)	0.98(4)	0.56(3)	0.04(2)	0.09(2)	0.03(2)
O(1)	1.0(2)	0.8(2)	0.5(2)	−0.2(2)	0.2(2)	−0.3(2)
O(2)	0.9(2)	1.1(2)	0.7(2)	0.2(2)	0.0(2)	0.2(2)
O(3)	1.0(2)	0.8(2)	0.6(2)	0.0(2)	0.2(2)	0.2(2)
O(4)	0.8(2)	1.0(2)	0.4(2)	−0.3(2)	−0.1(2)	0.1(2)

[a] B(iso) is the mean of the principal axes of the thermal ellipsoid.
[b] The Li atom was refined with isotropic temperature factor.
[c] Anisotropic temperature factors are of the form Tem = $\exp[-2\pi^2(h^2U_{11}a^{*2} + \cdots + 2hkU_{12}a^*b^* + \cdots)]$.

A view of the structure along the c-axis is shown in Fig. 3. It consists of corrugated layers of molybdenum oxide from the perovskite structure that share four O atom vertices within the layer and have terminal vertices above and below the layer. In the corrugated $MoO_2O_{4/2}$ layer, unlike the planar layer of K_2NiF_4, the two bonds from each equatorial O atom are nonlinear (Fig. 4a). The Sb^{3+} and Li^+ ions are segregated on opposite sides of each layer. Corrugated perovskite-like layers of LiO_6 octahedra are also formed by sharing the equatorial O

TABLE IV

SELECTED BOND DISTANCES (Å) AND ANGLES (°) FOR $LiSbMo_2O_8$

Bond distances			
Sb–O(3)[a]	2.982(5)	Sb–O(3)[b]	2.982(5)
Sb–O(3)	3.150(5)	Sb–O(3)[p]	3.150(5)
Sb–O(4)[c]	2.011(5)	Sb–O(4)[d]	2.208(5)
Sb–O(4)[e]	2.011(5)	Sb–O(4)[f]	2.208(5)
Mo–O(1)[g]	1.776(5)	Mo–O(1)[f]	2.208(5)
Mo–O(2)	1.729(5)	Mo–O(3)[d]	1.774(5)
Mo–O(3)[e]	2.210(5)	Mo–O(4)[h]	2.074(5)
Li–O(1)	2.150(5)	Li–O(1)[n]	2.150(5)
Li–O(2)[m]	2.155(5)	Li–O(2)[o]	2.155(5)
Li–O(2)[h]	2.097(5)	Li–O(2)[j]	2.097(5)
Bond angles			
O(4)[c]–Sb–O(4)[e]	92.2(2)	O(4)[c]–Sb–O(4)[f]	87.3(2)
O(4)[d]–Sb–O(4)[e]	87.3(2)	O(4)[d]–Sb–O(4)[f]	154.2(2)
O(4)[e]–Sb–O(4)[f]	74.8(2)	O(4)[e]–Sb–O(4)[d]	74.8(2)
Mo[i]–O(1)–Mo[j]	137.5(3)	Li[e]–O(2)–Li[h]	121.5(2)
Mo[d]–O(3)–Mo[k]	136.5(3)	Sb[m]–O(4)–Sb[d]	105.2(2)

Note. Symmetry codes: *a*, $-x, -y, -z$; *b*, $x, -y, 0.5 + z$; *c*, $-0.5 + x, 0.5 + y, z$; *d*, $0.5 - x, 0.5 - y, -z$; *e*, $0.5 - x, 0.5 + y, 0.5 - z$; *f*, $-0.5 + x, 0.5 - y, 0.5 + z$; *g*, $-0.5 + x, -0.5 + y, z$; *h*, $1 - x, y, 0.5 - z$; *i*, $0.5 + x, 0.5 + y, z$; *j*, $0.5 + x, 0.5 - y, -0.5 + z$; *k*, $0.5 - x, -0.5 + y, 0.5 - z$; *m*, $0.5 + x, -0.5 + y, z$; *n*, $1.5 - x, 0.5 - y, -z$; *o*, $1 - x, 1 - y, -z$ *p*, $-x, y, 0.5 - z$.

TABLE V

MOTIF OF MUTUAL ADJUNCTION, COORDINATION NUMBER (C.N.), AND BOND-ORDERS SUMS (Σs) IN $LiSbMo_2O_8$

	2 O(1)	2 O(2)	2 O(3)	2 O(4)	C.N.	Σs
Sb			4/2 (2.98 / 3.15 Å)[a]	4/2	4 (+4)	2.86 (3.07)
2 Mo	2/2	1/1	2/2	1/1	6	6.00
Li	2/1	4/2			6	0.99
C.N.	3	3	2 (+2)	3		
Σs	2.02	1.96	1.87 (1.98)	2.07		

[a] Long Sb–O distances are given in parentheses.

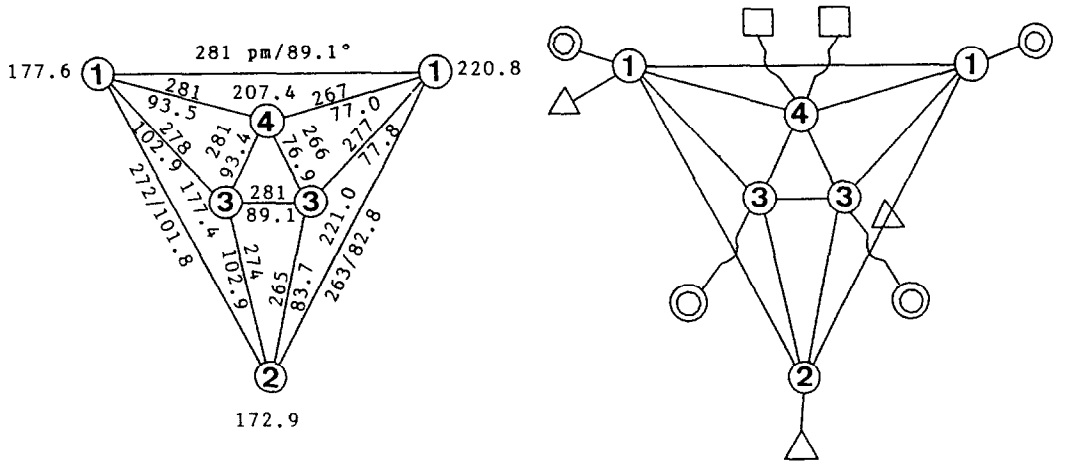

FIG. 1. Left, SCHLEGEL projection of a MoO_6 octahedron in $LiSbMo_2O_8$. The central Mo atom is not included in the projection. The Mo–O distances (pm) are given at the terminal positions of the projection. The O–O distances (pm) and their corresponding angles with respect to the central atom are indicated next to the edges. Estimated standard deviations on all O–MO–O angles are 0.2°. Right, SCHLEGEL diagram of the coordination polyhedron (C.P.) of O around Mo. Triangles are Li atoms; squares are Sb atoms; double circles are Mo atoms.

atom vertices (Fig. 4b). The Sb^{3+}–O polyhedra share edges to form infinite chains parallel to the *c*-axis with adjacent Sb^{3+} lone-pair orbitals within a chain pointing in opposite directions (Fig. 5). Interestingly, the projections down [010] and [102] show a rutile-type slab parallel to (100), which is made of a central Li–O layer sandwiched between two Mo–O layers (Fig. 6). These slabs are connected by the Sb^{3+} ions to give a three-dimensional framework.

It is noted that $LiSbMo_2O_8$, $SbNbO_4$ (*12*), the orthorhombic α, and the monoclinic β form of Sb_2O_4 (*13, 14*) are related

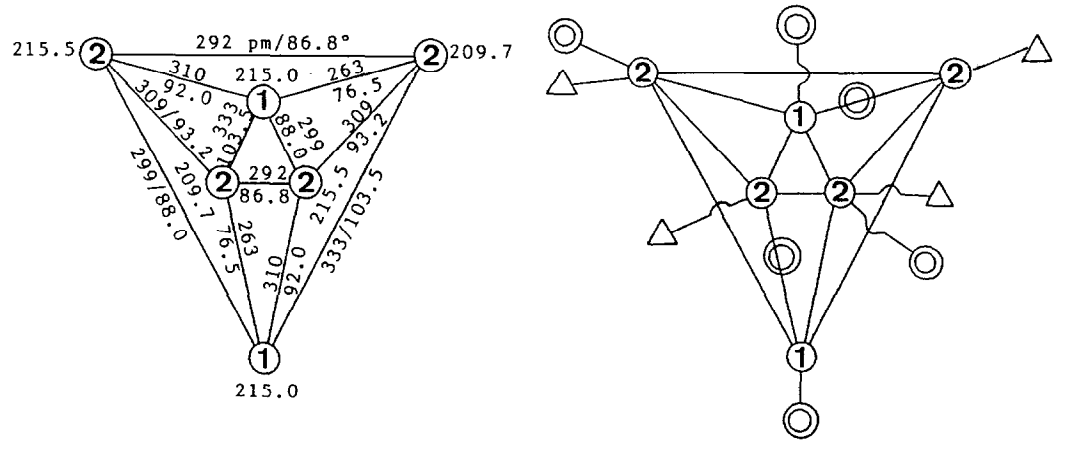

FIG. 2. Left, SCHLEGEL projection of a LiO_6 octahedron in $LiSbMo_2O_8$. Estimated standard deviations on all O–Li–O angles are 0.2°. Right, SCHLEGEL diagram of the C.P. of O around Li. Triangles are Li atoms; double circles are Mo atoms.

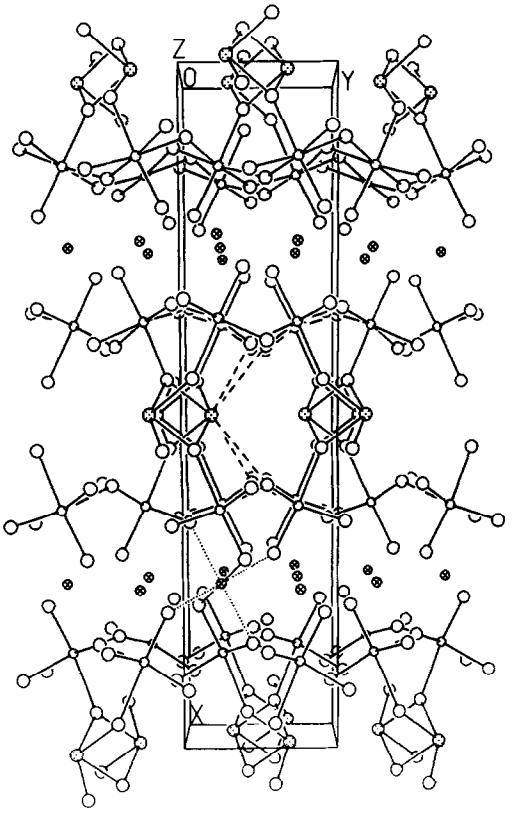

FIG. 3. A view of the structure of $LiSbMo_2O_8$ along the c-axis. The Li, Sb, Mo, and O atoms are represented by cross-hatched, dotted, small, and large open circles, respectively. The long Sb–O bonds are represented by dashed lines. The Li–O bonds are represented by dotted lines.

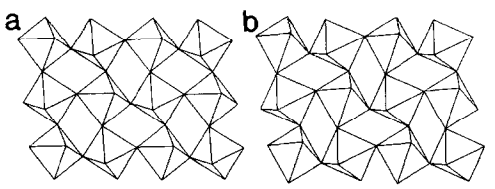

FIG. 4. (a) A polyhedron representation of a corrugated perovskite-like layer of MoO_6 octahedra. (b) A layer of LiO_6 octahedra.

structures. Both polymorphs of Sb_2O_4 ($=Sb^{3+}Sb^{5+}O_4$) consist of corrugated layers formed from $Sb^{5+}O_6$ octahedra sharing all their equatorial vertices and the Sb^{3+} ions lie between the layers in positions of one-sided 4-coordination. The Sb^{3+}–O polyhedra share edges to form infinite chains. Two essential differences between the two polymorphs are that in α-Sb_2O_4 the Sb^{5+}–O octahedra are more distorted, and alternate chains of Sb^{3+}–O polyhedra along c have an opposite tilt. $SbNbO_4$, which is isostructural with α – Sb_2O_4, consists of corrugated perovskite-like layers of NbO_6 octahedra joined by Sb^{3+} ions. The title compound can be derived from $SbNbO_4$ or Sb_2O_4 by replacing Nb^{5+} or Sb^{5+} with Mo^{6+}, and a half of the Sb^{3+} with Li^+. The octahedral coordination around Mo^{6+} in the title compound appears considerably more distorted than that for Nb^{5+} in $SbNbO_4$ (d(Nb–O) = 1.81–2.12 Å). Both $LiSbMo_2O_8$ and β-Sb_2O_4 crystallize in the space group $C2/c$ with alternate chains of Sb^{3+}–O polyhedra along the a-axis tilting in the same direction about c. The length of the repeating unit along the a-axis of the $LiSbMo_2O_8$ structure is about twice the value of the β-Sb_2O_4 structure, since one-half of the Sb^{3+} ions in β-Sb_2O_4 are substituted by Li^+ ions.

Although $SbNbO_4$ and $BiNbO_4$ (*15*) have related structures, $LiSbMo_2O_8$ and LiBi

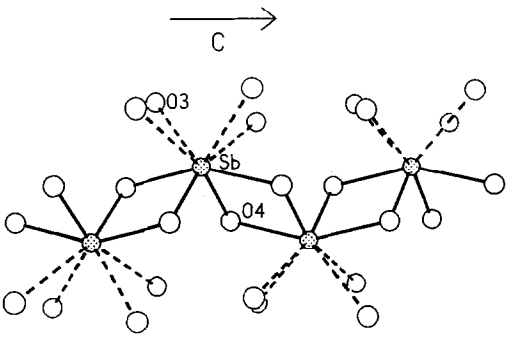

FIG. 5. A section of an infinite chain formed by edge-sharing Sb^{3+}–O polyhedra. The long Sb–O bonds are represented by dashed lines.

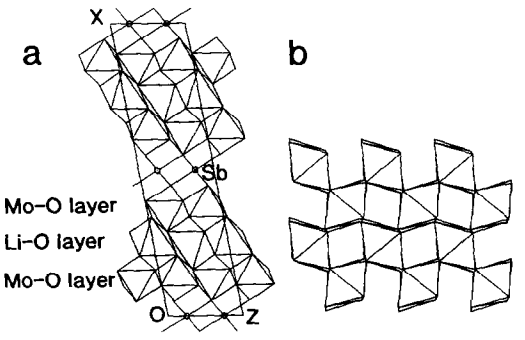

FIG. 6. (a) Projection of the structure of $LiSbMo_2O_8$ down [010] showing a rutile-type slab. (b) Projection of one slab down [10$\bar{2}$].

Mo_2O_8 (*16*) adopt two distinct structures, namely the β-Sb_2O_4 and scheelite types. It was reported that the compounds ABi Mo_2O_8 (A = alkali metals) (*16*) crystallize in four different structural types and are similar in their structures to the corresponding compounds of rare earths. It would be interesting to know whether there is any known isostructural compound among the corresponding antimony molybdates. Further research on the structural chemistry of ASb Mo_2O_8 is in progress.

Acknowledgments

Support for this study by the National Science Council and the Institute of Chemistry Academia Sinica is gratefully acknowledged. The authors thank Mr. Y. S. Wen for collecting single-crystal X-ray diffraction data and a referee for valuable comments.

References

1. A. LAARIF, F. R. THEOBALD, AND H. VIVIER, *Z. Kristallogr.* **167,** 117 (1984).
2. A. F. VAN DEN ELZEN AND G. D. RIECK, *Acta Crystallogr. Sect. B* **29,** 2436 (1973).
3. PAR M. PARMENTIER, C. GLEITZER, A. COURTOIS, AND J. PROTAS, *Acta Crystallogr. Sect. B* **35,** 1963 (1979).
4. K. H. LII, B. R. CHUEH, AND S. L. WANG, *J. Solid State Chem.* **86,** 188 (1990).
5. E. J. GABE, Y. LE PAGE, J.-P. CHARLAND, AND F. L. LEE, *J. Appl. Crystallogr.* **22,** 384 (1989).
6. D. T. CROMER AND J. T. WEBER, "International Tables for X-Ray Crystallography," Vol. IV. The Kynoch Press, Birmingham, England (1974).
7. R. HOPPE, *Angew. Chem. Int. Ed. Engl.* **19,** 110 (1980).
8. I. D. BROWN AND D. ALTERMATT, *Acta Crystallogr. Sect. B* **41,** 244 (1985).
9. R. D. SHANNON, *Acta Crystallogr. Sect. A* **32,** 751 (1976).
10. G. DONNAY AND R. ALLMANN, *Amer. Mineral.* **55,** 1003 (1970).
11. R. HOPPE AND J. KOEHLER, *Z. Kristallogr.* **183,** 77 (1988).
12. A. C. SKAPSKI AND D. ROGERS, *Chem. Commun.* 611 (1965).
13. G. THORNTON, *Acta Crystallogr. Sect. B* **33,** 1271 (1977).
14. D. ROGERS AND A. C. SKAPSKI, *Proc. Chem. Soc.*, 400 (1964).
15. B. AURIVILLIUS, *Arkiv Kemi* **3,** 153 (1951).
16. P. V. KLEVTSOV, V. A. VINOKUROV, AND R. F. KLEVTSOVA, *Sov. Phys. Crystallogr.* **18,** 749 (1974).